Microwave Spectra, Geometries, and Hyperfine Constants of OCCuX (X = F, Cl, Br)

Nicholas R. Walker and Michael C. L. Gerry*

Department of Chemistry, The University of British Columbia, 2036 Main Mall, Vancouver, British Columbia, Canada V6T 1Z1

Received June 6, 2001

A pulsed jet cavity Fourier transform microwave spectrometer has been used to measure the rotational spectra of OCCuX (X = F, Cl, Br) in the frequency range 5−21 GHz. Metal atoms were generated via laser ablation and were allowed to react with CO and a halide precursor, prior to stabilization of the products within a supersonic jet. These are the first experimental observations of OCCuF and OCCuBr and the first high-resolution spectroscopic study of gas-phase OCCuCl. All three molecules were found to be linear. Rotational constants, centrifugal distortion constants, nuclear quadrupole coupling constants, and nuclear spin-rotation coupling constants have been precisely determined. The rotational constants have been used to evaluate the various bond lengths, and the results are in good agreement with the trend established for OCAuX species. The C−O distance is found to be comparatively short and close to that of free CO. The M−C distance is longer than that predicted by ab initio calculations, and the Cu−X distances are very similar to those observed in the corresponding metal halides. Vibrational wavenumbers have been estimated from the distortion constants and are compared with the results of various ab initio studies. Changes in the Cu, Cl, and Br nuclear quadrupole coupling constants indicate that substantial charge rearrangement takes place on coordination with CO, consistent with the formation of strong Cu−C bonds. Mulliken orbital population analyses have been performed and provide evidence of π-back-donation from Cu in all of the species studied. The evaluated nuclear spin-rotation coupling constants have been used to estimate the ^{63}Cu nuclear shielding constants, σ, and their spans (Ω) in OC^{63}CuF, OC^{63}Cu^{35}Cl, and OC^{63}Cu^{79}Br.

I. Introduction

Recent work has demonstrated that relatively strongly bound species containing noble-gas and coinage-metal atoms are stabilized in a supersonic jet and can be interrogated by Fourier transform microwave (FTMW) spectroscopy. The first such species identified were ArAgX (X = F, Cl, Br),[1] which were shown to possess remarkably short and rigid Ar−Ag bonds. Later, the corresponding species ArCuX[2] and ArAuX[3,4] were also identified, as were KrAuCl,[3] KrAgCl,[5] and KrAgF.[6] Noble-gas−noble-metal chemical bonding was found in these compounds. Their existence suggests that the technique may be applicable to many similar species. One possibility replaces the noble gases with CO, to form compounds of the type OCMX (M = Cu, Ag, Au; X = F, Cl, Br).

An improved understanding of the bonding between transition metals and carbonyl groups is necessary in the context of our developing knowledge of transition-metal chemistry. Quantitative information, of the kind provided by microwave spectroscopy, is of central importance as a benchmark with which quantum-chemical predictions can be compared. Because microwave spectroscopy investigates isolated gas-phase molecules, geometries free of librational and other condensed-phase distortions can be obtained. Centrifugal distortion constants provide information relevant to the rigidity and vibrations of a molecule. Furthermore, hyperfine constants, most commonly arising through nuclear quadrupole coupling and/or nuclear spin-rotation coupling, are rationalized through the electronic characteristics of the molecule.

Although a vast range of transition-metal carbonyls exists, bonds between the coinage metals and CO are comparatively rare.[7] It is notable that, where bonds between copper(I) and CO are observed, it is frequently necessary for the compound to be sustained under an atmosphere of carbon monoxide. The infrared spectra of several group 11 carbonyls[7,8] all show the CO stretching frequency to be greater than that of free CO. These features have led to the suggestion that the conventional mechanism for metal−CO binding, where OC→M σ-donation is accompanied by synergistic M→CO π-back-donation, may not be appropriate for the coinage metals.[7]

Of the OCMX series of molecules (where M is an atom of group 11), only OCAuX (X = F, Cl, Br),[9−13] OCAgCl,[16] and OCCuCl[8,14] have been previously reported. Of these, OCAuCl

* To whom correspondence should be addressed. Fax: +1-604-822-2847. E-mail: mgerry@chem.ubc.ca.

(1) Evans, C. J.; Gerry, M. C. L. *J. Chem. Phys.* **2000**, *112*, 1321.
(2) Evans, C. J.; Gerry, M. C. L. *J. Chem. Phys.* **2000**, *112*, 9363.
(3) Evans, C. J.; Lesarri, A.; Gerry, M. C. L. *J. Am. Chem. Soc.* **2000**, *122*, 6100.
(4) Evans, C. J.; Rubinoff, D. S.; Gerry M. C. L. *Phys. Chem. Chem. Phys.* **2000**, *2*, 3943.
(5) Reynard, L. M.; Evans, C. J.; Gerry M. C. L. *Mol. Spectrosc.* **2001**, *206*, 33.
(6) Walker, N. R.; Reynard L. M.; Gerry, M. C. L. *J. Mol. Struct.* **2001** (accepted).
(7) Hurlburt, P. K.; Rack, J. J.; Luck, J. S.; Dec, S. F.; Webb, J. D.; Anderson, O. P.; Strauss, S. H. *J. Am. Chem. Soc.* **1994**, *116*, 10003.
(8) Plitt, H. S.; Bär, M. R.; Ahlrichs, R.; Schnöckel, H. *Inorg. Chem.* **1992**, *31*, 463.
(9) Karasch, M. S.; Isbell, M. S. *J. Am. Chem. Soc.* **1930**, *52*, 2919.
(10) Dell'Amico, D.; Calderazzo, F. *Gazz. Chim. Ital.* **1973**, *103*, 1099.
(11) Browning, J.; Goggin, P. L.; Goodfellow, R. J.; Norton, M. G.; Rattray, A. J. M.; Taylor, B. F.; Mink, J. *J. Chem. Soc., Dalton Trans.* **1977**, 2061.
(12) Dell'Amico, D.; Calderazzo, F.; Robino, P.; Segre, A. *J. Chem. Soc., Dalton Trans.* **1991**, 3017.
(13) Evans, C. J.; Reynard, L. M.; Gerry, M. C. L. *Inorg. Chem.* **2001**, in press.
(14) Hakansson, M.; Jagner, S. *Inorg. Chem.* **1990**, *29*, 5241.

10.1021/ic0105967 CCC: $20.00
Published on Web 10/18/2001

has long been known,[9] and is so stable that its crystal structure has been determined;[11] its crystals contain packed linear OCAuCl monomers. OCAuBr is less stable, and the first reports of it are only recent.[12] Microwave spectra of all three carbonyl gold halides have been recently observed and their geometries measured.[13] All have a C−O bond whose length is very close to that of free CO, as well as relatively long Au−C bonds.

Though aqueous acidic CuCl is well-known to absorb CO and has been used to assay CO gas,[15] it is also only recently that OCCuCl has been isolated as a solid well enough to determine its crystal structure. The solid has a polymeric layer structure, with each Cu(I) tetrahedrally coordinated to three Cl and one CO moieties.[14] Its infrared spectrum shows a CO stretching frequency slightly less than that of free CO, in contrast to most coinage metal carbonyls. However, monomeric OCCuCl has been isolated by condensing CO and CuCl in an Ar matrix.[8] Its infrared spectrum is consistent with that of a linear molecule, with a Cu−C bond; this time the CO stretching frequency is slightly greater than that of free CO. The method of matrix isolation has also been employed to generate OCAgCl, as reported recently by Shao et al.[16] The results again indicate that the molecule should be linear in the gas phase.

The chlorides OCMCl (M = Cu, Ag, Au), have been the subject of several ab initio studies.[8,16,17] Geometries, dissociation energies, stretching force constants, dipole moments, and ^{35}Cl nuclear quadrupole coupling constants have been predicted. All these studies conclude that there is some metal−CO π*-back-bonding, which would be inconsistent with a blue shift in the CO stretching frequency. Antes et al.[17] suggest that the blue shift may have an electrostatic origin. The structure and vibrational frequencies of OCCuF have also been the subject of theoretical calculation at the MP2 level.[18]

In this paper we present the pure rotational spectra of monomeric OCCuF, OCCuCl, and OCCuBr. This is the first report of any kind for for both the fluoride and the bromide. All three molecules were prepared by laser ablation of Cu in the presence of CO and a halogen precursor (SF_6, Cl_2 or Br_2) contained in the Ar backing gas of a supersonic jet. Rotational constants, centrifugal distortion constants, nuclear quadrupole coupling constants, and nuclear spin-rotation constants have been obtained, for many isotopomers of each molecule. Molecular geometries have been determined in all cases. The distortion constants are used to obtain vibrational information, and some insight into the electronic structures has been obtained from the hyperfine constants. Since the literature ab initio results refer only to the chloride, we have carried out corresponding calculations for all three molecules.

II. Experimental Methods

Experiments were conducted using a laser ablation system in conjunction with a Balle-Flygare[19] type Fourier transform microwave (FTMW) spectrometer. The system has been described at length in earlier papers;[20−22] therefore, only a brief description will be provided here. The microwave cavity consists of two spherical aluminum mirrors (28 cm diameter, radius of curvature 38.4 cm) separated by approximately 30 cm. One mirror is fixed, and the other is manually adjustable in order to permit the cavity to be tuned to the polarization frequency. The supersonic jet enters the cavity via a General Valve (Series 9) nozzle mounted slightly off-center in the fixed mirror. This arrangement optimizes the sensitivity and resolution of the spectrometer but causes all the lines to be observed as Doppler pairs, since the direction of microwave propagation is parallel to the direction of the supersonic jet. The line position is determined by finding the average frequency of the two Doppler components. All measurements are referenced to a Loran C frequency standard that is accurate to 1 part in 10^{10}.

The OCCuX molecules were generated via the laser ablation (Nd:YAG, 532 nm) of a copper rod (5 mm diameter, 98% purity) in the presence of a gas mixture containing halogen precursor, carbon monoxide, and argon. The rod was placed approximately 5 mm from the orifice of the pulsed nozzle and was simultaneously rotated and translated using a Motor Mike in order to expose a fresh surface of metal prior to each laser shot. The gas mixture for each experiment consisted of 0.1% of halogen-containing precursor (SF_6, Cl_2, or Br_2), 1.5% CO (Praxair), and argon. These concentrations were found to yield the most intense spectral lines for each of the molecules featured in this work. In order that experiments could be conducted on complexes containing ^{18}O and ^{13}C isotopes, isotopically enriched ^{13}CO and C^{18}O were employed.

III. Quantum Chemical Calculations

The geometries of OCCuF, OCCuCl, and OCCuBr were optimized at the second-order Møller−Plesset[23] level of theory using the GAUSSIAN 98[24] suite of programs. The vibrational wavenumbers and Mulliken orbital populations were calculated for each molecule. Calculations were also performed on the analogous metal halides (CuF, CuCl, and CuBr). The 6-311G** basis set[25] was used for the C, O, and F atoms. An effective core potential (ECP) was used for the copper atom, leaving 19 valence electrons ($3s^23p^63d^{10}4s^1$). The optimized Gaussian basis set (31111s/22111p/411d) and the effective core potential (ECP) were taken from Andrae et al.[26] The Cu basis set was augmented with two f-functions: $\alpha_f = 3.1235$ and $\alpha_f = 1.3375$.[17] The McLean−Chandler[27] basis set augmented with a d-polarization function[17] ($\alpha_d = 0.75$) was used for Cl (631111s/52111p). The calculations on OCCuCl, therefore, were performed using the same basis sets (and core potential for Cu) as were used by Antes et al. The aug-cc-pVTZ basis set was used for bromine.[28] This level of theory and these basis sets have been shown to give good agreement with experimental results obtained from a variety of ArMX and KrMX species.[1−6]

(15) *Comprehensive Coordination Chemistry*; Wilkinson, G., Ed.; Hathaway, B. J., Vol. Ed.; Pergamon: Oxford, U.K., 1987; Vol. 5 (Copper), pp 553−774.
(16) Shao, L.; Zhang, L.; Zhou, M.; Qin, Q. *Organometallics* **2001**, *20*, 1137.
(17) Antes, I.; Dapprich, S.; Frenking, G.; Schwerdtfeger, P. *Inorg. Chem.* **1996**, *35*, 2089.
(18) Bera, J. K.; Samuelson, G.; Chandrasekhar, J. *Organometallics* **1998**, *17*, 4136.
(19) Balle, T. J.; Flygare, W. H. *Rev. Sci. Instrum.* **1981**, *52*, 33.
(20) Xu, Y.; Jäger, W.; Gerry, M. C. L. J. *Mol. Spectrosc.* **1992**, *151*, 206.
(21) Brupbacher, Th.; Bohn, R. K.; Jäger, W.; Gerry, M. C. L.; Pasinszki, T.; Westwood, N. P. C. *J. Mol. Spectrosc.* **1997**, *181*, 316.
(22) Walker, K. A.; Gerry, M. C. L. *J. Mol. Spectrosc.* **1997**, *182*, 178.
(23) Møller, C.; Plesset, M. S. *Phys. Rev.* **1934**, *46*, 618.
(24) Frisch, M. J.; Trucks, G. W.; Schlegel, H. B.; Scuseria, G. E.; Robb, M. A.; Cheeseman, J. R.; Zakrzewski, V. G.; Montgomery, J. A., Jr.; Stratmann, R. E.; Burant, J. C.; Dapprich, S.; Millam, J. M.; Daniels, A. D.; Kudin, K. N.; Strain, M. C.; Farkas, O.; Tomasi, J.; Barone, V.; Cossi, M.; Cammi, R.; Mennucci, B.; Pomelli, C.; Adamo, C.; Clifford, S.; Ochterski, J.; Petersson, G. A.; Ayala, P. Y.; Cui, Q.; Morokuma, K.; Malick, D. K.; Rabuck, A. D.; Raghavachari, K.; Foresman, J. B.; Cioslowski, J.; Ortiz, J. V.; Stefanov, B. B.; Liu, G.; Liashenko, A.; Piskorz, P.; Komaromi, I.; Gomperts, R.; Martin, R. L.; Fox, D. J.; Keith, T.; Al-Laham, M. A.; Peng, C. Y.; Nanayakkara, A.; Gonzalez, C.; Challacombe, M.; Gill, P. M. W.; Johnson, B. G.; Chen, W.; Wong, M. W.; Andres, J. L.; Head-Gordon, M.; Replogle, E. S.; Pople, J. A. *Gaussian 98*, revision A.7; Gaussian, Inc.: Pittsburgh, PA, 1998.
(25) Krishnan, R.; Binkley, J. S.; Seeger, R.; Pople, J. A. *J. Chem. Phys.* **1980**, *72*, 650.
(26) Andrae, D.; Häusermann, V.; Dolg, M.; Stoll, H.; Preus, H. *Theor. Chim. Acta* **1990**, *77*, 123.
(27) McLean, A.; Chandler, G. S. *J. Chem. Phys.* **1980**, *72*, 5639.
(28) (a) Woon, D. E.; Dunning, T. H., Jr. *J. Chem. Phys.* **1993**, *98*, 1358. (b) Wilson, A. K.; Woon, D. E.; Peterson, K. A.; Dunning, T. H. Jr. *J. Chem. Phys.* **1999**, *110*, 7667.

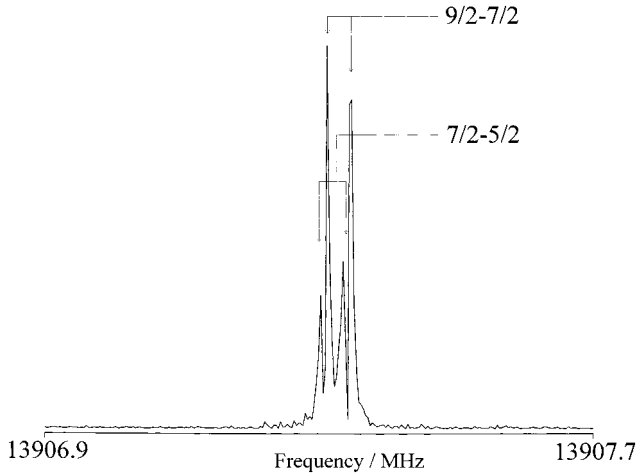

Figure 1. $F'-F'' = {}^7/_2 - {}^5/_2$ and $F'-F'' = {}^9/_2 - {}^7/_2$ transitions of $^{16}O^{12}C^{65}CuF$ ($J = 3-2$). Experimental conditions: 0.1% SF_6, 1.5% CO in argon, 300 averaging cycles, 4K data points, 4K transform.

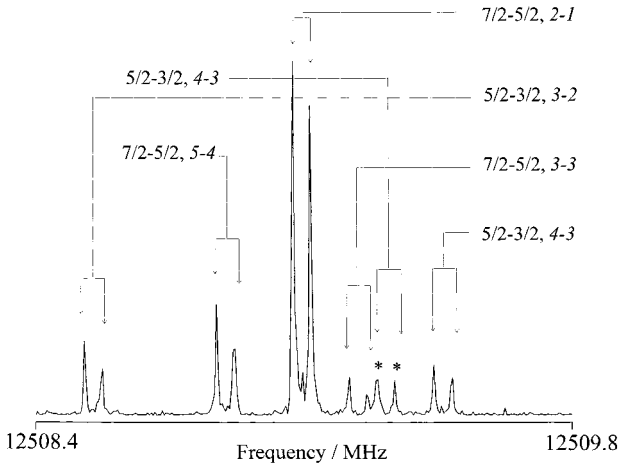

Figure 2. Hyperfine structure in the $J = 4-3$ transitions of $^{16}O^{12}C^{63}Cu^{35}Cl$ and $^{16}O^{12}C^{65}Cu^{35}Cl$ (indicated with an asterisk). Experimental conditions: 0.1% Cl_2, 1.5% CO in argon, 1000 averaging cycles, 4K data points, 4K transform. Quantum numbers $F_{Cu}'-F_{Cu}''$; $F'-F''$.

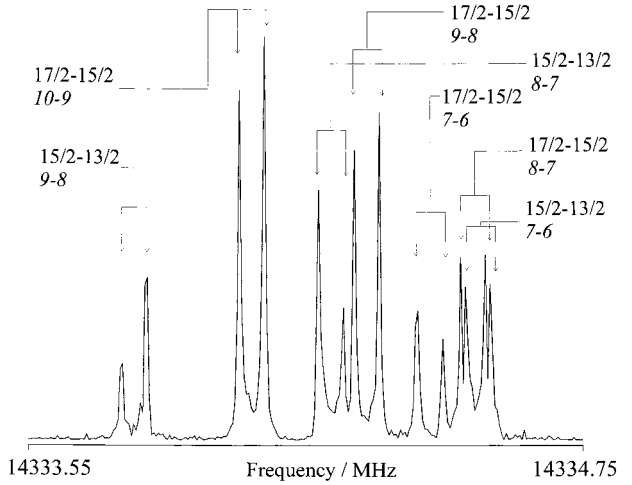

Figure 3. Hyperfine structure in the $J = 7-6$ transition of $^{16}O^{12}C^{63}Cu^{81}Br$ Experimental conditions: 0.1% Br_2, 1.5% CO in argon, 500 averaging cycles, 4K data points, 4K transform. Quantum numbers $F_{Br}'-F_{Br}''$; $F'-F''$.

IV. Assigned Spectra and Analyses

Recent work has shown that good agreement is obtained between MP2 calculated and experimentally determined structures for OCAuX molecules[13] (provided a suitable relativistic core potential is applied to the Au atom). Accordingly, an initial search for a spectrum of OCCuX, in particular of OCCuF, was based on such a prediction.

The first spectrum assigned during this work was that of the $OC^{63}CuF$ isotopomer. A line was identified at ~9297 MHz, which was around 320 MHz below the frequency predicted for the $J = 2-1$ transition. The spectrum was readily assigned and used to estimate the rotational constant of $OC^{65}CuF$. Lines from the spectrum of this isotopomer were also readily identified. The assignment was confirmed through comparison of the nuclear quadrupole coupling constants of the copper isotopes; their ratio was found to be very close to the ratio of the nuclear quadrupole moments of the two isotopes. An example of a doublet of OCCuF is shown in Figure 1. The lines were observed to be quite intense, and the strongest signals could be distinguished from the background noise after 20 averaging cycles.

The information derived from these initial studies of OCCuF included a comparatively accurate estimate of its geometry. The assumption was then made that the ratio of the Cu−C distances in OCCuF and OCCuCl would be similar to that of the Ar−Cu distances in the ArCuX series. Together with the assumption that the Cu−Cl distance would be similar to that of monomeric CuCl, this permitted the rotational constant of OCCuCl to be predicted. A search for lines in the spectrum of this molecule revealed lines for $J = 3-2$ within 50 MHz of the position initially predicted. Lines from $OC^{63}CuCl$ and $OC^{65}CuCl$ (for a given combination of oxygen, carbon, and chlorine isotopes) were observed to be heavily overlapped and were recorded simultaneously (Figure 2). The assignment of lines to the correct isotopomer was therefore nontrivial and time-consuming but was again confirmed through the ratio of the Cu nuclear quadrupole coupling constants. The close proximity of spectra of isotopomers containing different Cu isotopes indicates that the Cu atom is very close to the center of mass in the molecule. The most intense lines of OCCuCl could be identified after fewer than 20 averaging cycles.

The initial frequency search range for OCCuBr was determined using the same criteria as for OCCuCl: (i) the fractional change in the Cu−C bond between OCCuX molecules on X substitution was assumed to be the same as for Ar−Cu in ArCuX and (ii) the Cu−Br length was assumed to be equal to that in diatomic CuBr. Lines for $J = 6-5$ were identified within 100 MHz of their predicted frequencies, and the spectra of all four isotopomers (containing $^{63/65}Cu$ and $^{79/81}Br$) were assigned with little difficulty. The transitions of OCCuBr were less intense than those of OCCuF and OCCuCl, requiring in general double the averaging cycles for accurate line measurement. Several lines from the $J = 7-6$ transition of the $OC^{63}Cu^{81}Br$ spectrum are shown in Figure 3.

To obtain accurate geometries, spectra of isotopomers artificially enriched with ^{13}C and ^{18}O were measured, for all of these molecules. The range of data obtained using these species was smaller than that for those containing normal CO. For OCCuCl, data were collected from only one isotopomer containing $C^{18}O$, because the spectra were heavily overlapped.

Hyperfine structure due to ^{63}Cu and ^{65}Cu was observed for all three molecules. In addition, the chloride and bromide also showed $^{35}Cl/^{37}Cl$ and $^{79}Br/^{81}Br$ splittings. Since all six of these nuclei have $I = {}^3/_2$, the main cause was nuclear quadrupole coupling in each case. The quantum number assignments used the following schemes: for OCCuF, $\mathbf{J} + \mathbf{I}_{Cu} = \mathbf{F}$; for OCCuCl, $\mathbf{J} + \mathbf{I}_{Cu} = \mathbf{F}_1$ and $\mathbf{F}_1 + \mathbf{I}_{Cl} = \mathbf{F}$; for OCCuBr, $\mathbf{J} + \mathbf{I}_{Br} = \mathbf{F}_1$; and $\mathbf{F}_1 + \mathbf{I}_{Cu} = \mathbf{F}$. Measured line frequencies and their

Table 1. Molecular Constants (MHz) Calculated for Various Isotopomers of OCCuF

param	$^{16}O^{12}C^{63}CuF$	$^{16}O^{12}C^{65}CuF$
B_0	2 320.096 376(97)[a]	2 318.030 754(106)
$D_J \times 10^4$	2.641(26)	2.587(31)
eQq(Cu)	75.406(19)	69.790(14)
C_l(Cu) $\times 10^3$	10.13(16)	10.99(21)
param	$^{16}O^{13}C^{63}CuF$	$^{16}O^{13}C^{65}CuF$
B_0	2 298.036 954(76)	2 295.838 831(201)
$D_J \times 10^4$	2.616(48)	2.907(42)
eQq(Cu)	75.503(26)	69.835(31)
C_l(Cu) $\times 10^3$	10.73(58)	10.72(70)
param	$^{18}O^{12}C^{63}CuF$	$^{18}O^{12}C^{65}CuF$
B_0	2 188.369 970(180)	2 185.955 276(96)
$D_J \times 10^4$	2.286(39)	2.587[b]
eQq(Cu)	75.489(29)	68.864(54)
C_l(Cu) $\times 10^3$	11.82(68)	10.987[b]

[a] Numbers in parentheses are one standard deviation in units of the last significant figure. [b] Fixed to $^{16}O^{12}C^{65}CuF$ value.

assignments according to these coupling schemes are in the Supporting Information.

Pickett's global least-squares fitting program SPFIT[29] was used to fit the measured positions of spectral lines to a model Hamiltonian for the system

$$\mathbf{H} = \mathbf{H}_{\mathrm{rot}} + \mathbf{H}_{\mathrm{quad}} + \mathbf{H}_{\mathrm{spin-rot}} \tag{1}$$

where

$$\mathbf{H}_{\mathrm{rot}} = B_0\mathbf{J}^2 - D_J\mathbf{J}^4 \tag{2}$$

$$\mathbf{H}_{\mathrm{elec\ quad}} = \frac{1}{6}(\mathbf{V}_{\mathrm{Cu}}^{(2)}\,\mathbf{Q}_{\mathrm{Cu}}^{(2)} + \mathbf{V}_{\mathrm{X}}^{(2)}\,\mathbf{Q}_{\mathrm{X}}^{(2)}) \tag{3}$$

$$\mathbf{H}_{\mathrm{nucl\ spin-rotation}} = C_l(\mathrm{Cu})\mathbf{I}_{\mathrm{Cu}}\cdot\mathbf{J} \tag{4}$$

The rotational constant (B_0) and nuclear quadrupole coupling constants (eQq(Cu) and eQq(X)) were fit for every isotopomer of every molecule studied (except eQq(F) = 0). The distortion constant D_J and the copper nuclear spin-rotation constant C_l(Cu) were also fit for every isotopomer, with three exceptions: (i) for $^{18}O^{12}C^{65}Cu^{81}Br$, where only one $J'-J''$ transition had been measured, both these constants were fixed at the values for $^{16}O^{12}C^{65}Cu^{81}Br$; (ii) C_l(Cu) and D_J for $^{18}O^{12}C^{65}CuF$, being poorly determined, were fixed at their values in $^{16}O^{12}C^{65}CuF$; (iii) D_J for $^{16}O^{12}C^{65}Cu^{37}Cl$ was fixed at its value for $^{16}O^{12}C^{65}Cu^{35}Cl$. Since the halogen spin-rotation constants and the Cu−X spin−spin constants were indeterminate, they were excluded from the analysis. The resulting fit parameters are given in Tables 1−3 for OCCuF, OCCuCl, and OCCuBr, respectively.

Microwave spectra for vibrationally excited states of OCCuX species were not assigned during this work. During studies of OCCuCl, five lines were observed at frequencies between 9363 and 9373 MHz, approximately 15 MHz below the most intense lines of the ground state of $^{16}O^{12}C^{63}Cu^{35}Cl$. They could not be assigned to a ground-state spectrum of any isotopomer of OCCuCl and it is therefore probable that they originate from a vibrationally excited state of the species. Quantum numbers were not assigned. No evidence of lines from excited states of OCCuF and OCCuBr was found. This is consistent with the recent study of OCAuX species, for which excited states could be assigned only to OCAuCl.[13]

V. Structures of the Complexes

A. Structural Calculations. The level of precision of the measured line frequencies is one of the principal advantages of FTMW spectroscopy. Since these frequencies can typically be determined with an accuracy of ±1 kHz, the determined rotational constants are comparably precise; for OCCuX there are nine significant figures. Unfortunately, this precision is not carried over to derived bond distances, because of vibrational effects which are difficult to predict. The most precise structure is the equilibrium (r_e) structure, at the minimum of the potential well. It has the advantage of being isotopically independent (to an excellent approximation) and of being the parameter predicted in ab initio calculations. Unfortunately it requires rotational constants for many isotopomers in excited vibrational states, which are not available here. Structures must instead be obtained by rather approximate methods, which at least give qualitatively unique chemical information but for which much of the precision of the rotational constants is lost. In the present case, three methods were used.

i. Ground-State Effective (r_0) Structures. This method ignores any vibrational contributions to the rotational constants and moments of inertia of the ground vibrational state.[30] It assumes that rigid rotor formulas apply to the ground vibrational state. The bond lengths were thus fit by least squares to the moments of inertia I_0 derived directly from the rotational constants in Tables 1−3, using $I_0 = h/8\pi^2B_0$:

$$I_0 = I_{\mathrm{rigid}}(r_0) \tag{5}$$

The bond lengths are designated r_0, and $I_{\mathrm{rigid}}(r_0)$ is calculated from them using rigid-molecule formulas. The derived values for each molecule are given in Table 4.

Table 2. Molecular Constants (MHz) Calculated for Various Isotopomers of OCCuCl

param	$^{16}O^{12}C^{63}Cu^{35}Cl$	$^{16}O^{12}C^{65}Cu^{35}Cl$	$^{16}O^{12}C^{63}Cu^{37}Cl$	$^{16}O^{12}C^{65}Cu^{37}Cl$
B_0	1 563.426 847(41)[a]	1 563.422 003(89)	1 525.328 406(61)	1 525.299 017(56)
$D_J \times 10^4$	1.2960(85)	1.3215(269)	1.1933(161)	1.3215[b]
eQq(Cl)	-21.4735(22)	−21.4773(37)	−16.9111(31)	−16.9697(90)
eQq(Cu)	70.8323(210)	65.5635(44)	70.8325(55)	65.5605(67)
C_l(Cu) $\times 10^3$	6.057(93)	5.876(181)	5.989(155)	4.969(273)
param	$^{16}O^{13}C^{63}Cu^{35}Cl$	$^{16}O^{13}C^{65}Cu^{35}Cl$	$^{16}O^{13}C^{63}Cu^{37}Cl$	$^{18}O^{12}C^{63}Cu^{35}Cl$
B_0	1 547.587 01(15)	1 547.588 03(20)	1 509.723 21(21)	1 484.483 99(22)
$D_J \times 10^4$	1.299(50)	1.151(75)	1.254(67)	1.228(50)
eQq(Cl)	-21.4816(67)	−21.481(12)	−16.949(16)	−21.6153(33)
eQq(Cu)	70.868(15)	65.551(18)	70.8413(25)	71.0707(63)
C_l(Cu) $\times 10^3$	6.039(313)	5.80(56)	5.67(45)	7.06(38)

[a] Numbers in parentheses are one standard deviation in units of the last significant figure. [b] Fixed to D_J of $^{16}O^{12}C^{65}Cu^{35}Cl$.

Table 3. Molecular Constants (MHz) Calculated for Various Isotopomers of OCCuBr

param	$^{16}O^{12}C^{63}Cu^{79}Br$	$^{16}O^{12}C^{65}Cu^{79}Br$	$^{16}O^{12}C^{63}Cu^{81}Br$	$^{16}O^{12}C^{65}Cu^{81}Br$
B_0	1 034.112 397(37)[a]	1 032.564 157(46)	1 023.909 030(34)	1 022.298 736(48)
$D_J \times 10^4$	0.6158(40)	0.6099(57)	0.6050(36)	0.6022(60)
eQq(Cu)	67.534(12)	62.463(24)	67.503(18)	62.431(29)
C_l(Cu) $\times 10^3$	3.57(14)	3.67(15)	3.49(13)	3.87(16)
eQq(Br)	171.600(18)	171.558(29)	143.318(21)	143.265(32)
param	$^{16}O^{13}C^{63}Cu^{79}Br$	$^{16}O^{13}C^{65}Cu^{79}Br$	$^{16}O^{13}C^{63}Cu^{81}Br$	$^{16}O^{13}C^{65}Cu^{81}Br$
B_0	1 021.975 547(50)	1 020.533 051(68)	1 011.829 585(43)	1 010.327 107(61)
$D_J \times 10^4$	0.6115(52)	0.5982(86)	0.5994(44)	0.5902(80)
eQq(Cu)	67.453(45)	62.433(40)	67.546(16)	62.505(46)
C_l(Cu) $\times 10^3$	3.19(19)	2.89(20)	3.85(16)	3.78(24)
eQq(Br)	171.525(55)	171.585(52)	143.350(26)	143.357(45)

param	$^{18}O^{12}C^{63}Cu^{79}Br$	$^{18}O^{12}C^{63}Cu^{81}Br$	$^{18}O^{12}C^{65}Cu^{81}Br$
B_0	984.114 293(62)	974.380 464(49)	973.106 627(35)
$D_J \times 10^4$	0.5481(60)	0.5347(49)	0.6022[b]
eQq(Cu)	67.504(35)	67.507(25)	62.329(69)
C_l(Cu) $\times 10^3$	3.11(28)	3.57(22)	3.87[b]
eQq(Br)	171.493(58)	143.208(47)	143.093(74)

[a] Numbers in parentheses are one standard deviation in units of the last significant figure. [b] Fixed to $^{16}O^{12}C^{65}Cu^{81}Br$ value.

Table 4. Experimental and ab Initio Bond Lengths (Å) for OCCuX

method	r(CO)	r(CCu)	r(CuX)
		OCCuF	
r_0	1.1307(2)[a]	1.7639(4)	1.7364(3)
$r_{I\epsilon}$	1.13078(3)	1.76455(6)	1.7332(2)
$r_m^{(1)}$	1.13033(3)	1.76385(4)	1.7325(3)
MP2[b]	1.145	1.708	1.713
MP2[c]	1.154	1.774	1.711
		OCCuCl	
r_0	1.128(1)	1.796(1)	2.0558(7)
$r_{I\epsilon}$	1.12872(7)	1.79493(9)	2.05480(5)
$r_m^{(1)}$	1.12818(7)	1.7940(1)	2.05379(7)
$r_m^{(2)}$	1.12755(1)	1.79447(1)	2.053419(8)
MP2[b]	1.143	1.735	2.042
MP2[d]	1.143	1.725	2.033
MP2[e]	1.137	1.750	2.047
DFT[f]	1.129	1.826	2.096
CPF[e]	1.128	1.807	2.070
		OCCuBr	
r_0	1.1277(6)	1.8022(9)	2.182(4)
$r_{I\epsilon}$	1.12821(8)	1.8027(1)	2.1797(1)
$r_m^{(1)}$	1.12775(8)	1.8019(1)	2.1788(1)
$r_m^{(2)}$	1.12721(2)	1.80238(2)	2.17871(1)
MP2[b]	1.143	1.745	2.149

[a] Numbers in parentheses are one standard deviation in units of the last significant figure. [b] This work. [c] Reference 18. [d] Reference 17. [e] Reference 8. [f] Reference 16.

ii. Fitted Substitution ($r_{I\epsilon}$) Structures. This method makes some allowance for vibrational contributions to I_0, by fitting the bond lengths to

$$I_0 = I_{\text{rigid}}(r_{I\epsilon}) + \epsilon \qquad (6)$$

where ϵ is a vibration−rotation correction to I_0 and thus an additional fitting parameter. It is assumed to be independent of isotopomer.[31] This assumption is also made in the conventional substitution (r_s) method,[32] in which a basis molecule is chosen and atomic positions are determined by making isotopic substitutions at each atom. Where principal moments of several isotopic species have been obtained (as in the present case), the resulting structures should be the same.

The $r_{I\epsilon}$ values for each molecule are also given in Table 4. Since ϵ compensates at least in part for vibration−rotation contributions to I_0, the $r_{I\epsilon}$ values are an order of magnitude better determined than the r_0 values.

iii. Mass-Dependent $r_m^{(1)}$ and $r_m^{(2)}$ Geometries. To obtain these geometries, an effort is made to account for the mass dependence of ϵ (ie its dependence on isotopic species) using the equation[33]

$$I_0 = I_m(r_m) + cI_{\text{m}}^{1/2} + d((m_1m_2m_3m_4)/M)^{1/6} \qquad (7)$$

where r_m are the derived bond lengths, $I_m(r_m) = I_{\text{rigid}}(r_m)$ is the moment of inertia derived from them with rigid rotor formulas, and c and d are new fitting constants. In an $r_m^{(1)}$ fit d is set to zero; in an $r_m^{(2)}$ fit both c and d are included as fit parameters. The r_m structures, particularly $r_m^{(2)}$, provide probably the best approximations to equilibrium (r_e) structures as can be obtained from ground vibrational state data alone.

The derived $r_m^{(1)}$ and $r_m^{(2)}$ values are also given in Table 4. Only an $r_m^{(1)}$ value was obtained for OCCuF. Since both the $r_m^{(1)}$ and $r_{I\epsilon}$ methods fit to one constant besides the bond lengths, the precision of the bond lengths is the same in both cases. For the OCCuX molecules the $r_m^{(2)}$ values are up to an order of magnitude better determined. This is perhaps to be expected, since the $r_m^{(2)}$ values give the best representation of the mass dependence of ϵ. They are our preferred values. However, as has been found in other cases,[13] especially where there are no atoms near the center of mass, the bond lengths are strongly correlated; therefore, they must be viewed cautiously.

B. Evaluated Structural Parameters. The results of structural fits are presented alongside the predictions of various theoretical methods in Table 4. The bond lengths determined by experiment for OCCuX are considerably different from those predicted by the most recent MP2 and DFT calculations. This is somewhat unexpected, given the accuracy obtained earlier using MP2 calculations on OCAuX, ArCuX, ArAgX, ArAuX, KrAgX, and KrAuCl performed at the same level of theory and using the same basis sets. Experimental data and the results of

(29) Pickett, H. M. *J. Mol. Spectrosc.* **1991**, *148*, 371.
(30) Gordy, W.; Cook, R. L. *Microwave Molecular Spectra*, 3rd ed.; Techniques of Chemistry XVIII; Wiley: New York, 1984.
(31) Rudolph, H. D. *Struct. Chem.* **1991**, *2*, 581.
(32) Costain, C. C. *J. Chem. Phys.* **1958**, *29*, 864.
(33) Watson J. K. G.; Roytburg, A.; Ulrich. W. *J. Mol. Spectrosc.* **1999**, *196*, 102.

Table 5. Experimental and ab Initio Bond Lengths (Å) of CuX

	CuX	
	MP2	exptl (r_e)
CuF	1.735	1.745[a]
CuCl	2.049	2.051[b]
CuBr	2.154	2.173[c]

[a] Hoeft, J; Lovas, F. J.; Tiemann, E.; Törring, T. *Z. Naturforsch.* **1970**, *25a*, 35. [b] Manson, E. L.; De Lucia, F. C.; Gordy. W. *J. Chem. Phys.* **1975**, *62*, 1040. [c] Manson, E. L.; De Lucia, F. C.; Gordy. W. *J. Chem. Phys.* **1975**, *63*, 2724.

our own theoretical calculations on the diatomic copper halides are presented in Table 5; in all cases, it can be seen that good agreement is obtained. The DFT results of Shao et al.[16] are in good agreement with the experimental data for the C−O and Cu−C distances in OCCuX species; however, the CuX distance has been significantly overestimated. The results of Plitt et al.[8] are the most consistent with experiment. Those obtained using the CPF method give the best agreement, though the results of their MP2 calculations are also reasonably accurate.

In every case, the change in CuX bond distance on attachment of CO is comparatively small for each metal halide. While the Cu−F distance in OCCuF is significantly shorter than that in CuF (by between 0.01 and 0.02 Å), little change is observed in the Cu−X ($r_m^{(2)}$) distance in the formation of both OCCuCl and OCCuBr. The MP2 calculations predict (in general) that a small decrease should be observed. It is interesting to note that a similar behavior is observed in ArCuX species: though MP2 calculations predict that the Cu−X bond length should decrease on attachment of an argon atom to a copper halide molecule, no significant change is seen. The experimental $r_m^{(2)}$ Cu−Cl distance is observed to be ∼0.005−0.02 Å longer than the results of the various MP2 calculations but is 0.02 Å shorter than the distance predicted by a CPF method and 0.04 Å shorter than predicted by DFT. The Cu−F and Cu−Br distances in OCCuF and OCCuBr, are observed to be 0.02 and 0.03 Å longer, respectively, than predicted by the MP2 calculation (CPF results are not available for these species).

Most of the MP2 calculations significantly underestimate the Cu−C distance in each of the species studied. In the case of OCCuF, the magnitude of the discrepancy is ∼0.05 Å for the calculation performed during this work. The result of Bera et al.[18] is 0.01 Å higher than the experimental value. The difference is ∼0.04 to ∼0.07 Å for OCCuCl and is ∼0.06 Å for OCCuBr. The CPF result is in much better agreement; it overestimates the distance by ∼0.01 Å. The experimentally determined ($r_m^{(2)}$) C−O distance in OCCuX approaches that of uncoordinated carbon monoxide (1.128 Å). It is apparent that the MP2 calculations give distances that are generally between 0.01 and 0.02 Å too long, though it is notable that the MP2 calculated bond length of carbon monoxide is also overestimated by 0.01 Å. The CPF calculation for OCCuCl reproduces the experimental value very well, as does the value obtained using DFT (±0.001 Å).

The respective fractional changes in the Cu−C and C−O distances on substitution of the halogen atom in OCCuX are considerably greater where the substitution replaces fluorine with chlorine rather than chlorine with bromine. This behavior is also present in the bond lengths determined through theoretical calculation. The same phenomenon was also found for the corresponding OCAuX complexes.[13]

VI. Vibrational Frequencies

The distortion constant of a molecule provides an indication of the rigidity of its bonds and is therefore intimately connected to its vibration frequencies. The lowest frequency stretching vibration of each OCCuX molecule was estimated from its distortion constant by using a pseudodiatomic approximation:

$$\omega \approx \left(\frac{4B_0^3}{D_J}\right)^{1/2} \tag{8}$$

The result of this calculation for each molecule is shown alongside various theoretical results in Table 6. In each case, the distortion constant chosen was that of the most abundant isotopomer.

Table 6. Experimental and ab Initio Vibrational Wavenumbers of OCCuX (cm^{-1})

	method	Σ CO str	Σ MC str	Π MCO def	Σ MX str	Π XMC def	exptl[a,b]
OCCuF	MP2[b]	2105.5	512.5	466.4	731.3	129.6	468
OCCuCl	MP2[b]	2108.7[c]	559.3	427.7	399.7[d]	92.6	362
	MP2[e]	2104.4[c]	572.9	437.0	407.0[d]	92.4	
	DFT[f]	2212[c]	485	369	345[d]	78	
	CPF[g]	2144[c]	580	442	389[d]	103	
OCCuBr	MP2[b]	2097.9	532.0	416.2	307.6	79.1	283

[a] Value obtained from the centrifugal distortion constant using the diatomic approximation (eq 8). [b] This work. [c] Experimental value[8] is 2156.5 cm^{-1}. [d] Experimental value from the matrix infrared spectrum[8] is 361.6 cm^{-1}. [e] Reference 17. [f] Reference 16. [g] Reference 8.

Several theoretical results are available for OCCuCl, permitting the variation in the calculated frequencies to be examined with reference to the different methods and basis sets employed. It can be seen that the CO stretching mode shows very little variation (all values are between 2104.4 and 2212 cm^{-1}); the greatest variation is present in the values for the Π XMC bend. The remaining modes (MC stretch, MX stretch, and MCO bend) show fractional variations which lie midway between these two extremes. The value determined from the experimental distortion constant is expected to approximate the lowest frequency stretch; in OCCuCl this is predicted to be the Σ MCl stretch. Its ab initio values all fall within the range from 345 to 407 cm^{-1}, while the value determined from the distortion constant is 362 cm^{-1}. Our experimental result is consistent with both the matrix IR spectrum and the CPF value determined by Plitt et al.[8] It should be noted that the CPF method was also found to produce the best agreement with the experimental geometry. The DFT result obtained by Shao et al.[16] is in good agreement with the experimental data. The results of the MP2 calculations are reasonably close to, though somewhat higher than, the value obtained from the distortion constant.

In the case of OCCuF and OCCuBr, the MP2 calculations performed during this work offer the only available comparison with the experimental results. As was the case with OCCuCl, the lowest frequency stretch of OCCuBr is predicted to be the CuX stretch (307.6 cm^{-1}). This prediction is 24 cm^{-1} higher than the result calculated from the distortion constant (283 cm^{-1}). The level of agreement with the measured distortion constant is therefore very similar to that observed in OCCuCl, allowing for the slightly different magnitudes of the respective stretching frequencies. The lowest frequency stretch of OCCuF is predicted to be the MC stretch. The ab initio prediction of the frequency of this mode is 512.5 cm^{-1}, which is 44.5 cm^{-1} higher than the value obtained from the distortion constant (468 cm^{-1}). Again, the level of agreement is very similar to that observed between the results of our MP2 calculations and the distortion constants of OCCuCl and OCCuBr.

Table 7. Experimental and ab Initio Vibrational Wavenumbers (cm^{-1}) of CuX

	MP2	exp
CuF	625.1745	621.5[a]
CuCl	429.0320	417.6[b]
CuBr	330.9729	313.1[c]
CO	2134.1	2138[d]

[a] Ahmed, F.; Barrow, R. F.; Chojnicki, A. H.; Dufour, C.; Schamps, J. *J. Phys. B* **1982**, *15*, 3801. [b] Manson, E. L.; De Lucia, F. C.; Gordy, W. *J. Chem. Phys.* **1975**, *62*, 1040. [c] Manson, E. L.; De Lucia, F. C.; Gordy, W. *J. Chem. Phys.* **1975**, *63*, 2724. [d] Huber, K. P.; Herzberg, G. *Molecular Spectra and Molecular Structure Constants of Diatomic Molecules*; Van Nostrand: New York, 1979.

Table 8. Nuclear Quadrupole Coupling Constants of Cu, Cl, and Br in OCCuX, CuX, ArCuX, and $[XCuX]^-$ in MHz

	$eQq(^{63}Cu)$			
X[a]	OCCuX[b]	CuX	ArCuX[c]	$[XCuX]^-$
F	75.406	21.956[c]	38.055	
Cl	70.832	16.169[d]	33.186	61.4[e]
Br	67.534	12.851[d]	29.923	57.7[f]

	eQq(X)			
X[a]	OCCuX[b]	CuX	ArCuX[c]	$[XCuX]^-$
Cl	−21.474	−32.127[d]	−28.032	−19.3[e]
Br	171.600	261.180[d]	225.554	152.8[f]

[a] Data are for ^{19}F, ^{35}Cl, and ^{79}Br isotopes, respectively. [b] This work. [c] Reference 2. [d] Low, R. J.; Varberg, T. D.; Connelly, J. P.; Auty, A. P.; Howard, B. J.; Brown, J. M. *J. Mol. Spectrosc.* **1993**, *161*, 499. [e] Bowmaker, G. A.; Brockliss, L. D.; Whiting, R. *Aust. J. Chem.* **1973**, *26*, 29. [f] Bowmaker, G. A.; Boyd, P. D. W.; Sorrenson, R. J. *J. Chem. Soc., Faraday Trans. 2* **1985**, *81*, 1627.

VII. Hyperfine Coupling

The spectra of all three complexes contain hyperfine structure caused by coupling of the nuclear spins of Cu, Cl, and Br with the rotation of the molecules. Since all these nuclei have $I = {}^3/_2$, nuclear quadrupole coupling is predominant. This coupling arises through an electric field gradient (EFG) at the nucleus and, hence, gives a measure of the electron distribution and the bonding of the given atom. Any significant variation in the electronic structure, for example through the formation of a new chemical bond, will result in a change in the EFG of the quadrupolar nucleus and its associated nuclear quadrupole coupling constant, eQq. Magnetic spin-rotation coupling of Cu has also been observed for all the complexes. Although it is small, it is apparently real. It arises through a mechanism very similar to nuclear shielding in nuclear magnetic resonance (NMR) and permits shielding parameters to be estimated.

A. Nuclear Quadrupole Coupling Constants. Table 8 contains the ^{63}Cu nuclear quadrupole coupling constants for all the OCCuX molecules, along with those of the CuX dimers, ArCuX complexes, and the $[XCuX]^-$ ions. There are major changes in the ^{63}Cu coupling constant when CO attaches to CuX. These changes are roughly the same for all three halides, though it is slightly smaller for the fluoride.

They are considerably greater than the changes on addition of Ar to the halides and even greater than those on formation of the $[XCuX]^-$ ions. They roughly parallel the changes found for the equivalent Au complexes.[13] However, the distinct difference found between OCAuF and the other two Au complexes is not reproduced for Cu. Table 8 also contains a comparison for the ^{35}Cl and ^{79}Br coupling constants. For both nuclei the magnitudes of the coupling constants decrease significantly, consistent with electron donation from CO to CuX on complex formation. Though the change is once again considerably greater than that on formation of ArCuX, it is this time less than that found on formation of $[XCuX]^-$ ions. These observations parallel those made for the corresponding Au complexes.

Table 9. MP2 Mulliken Orbital Populations for OCCuX

	FCuCO	CuF + CO	ClCuCO	CuCl + CO	BrCuCO	CuBr + CO
q^X	−0.61	−0.64	−0.46	−0.49	−0.42	−0.50
n_s^X	2.00	2.00	1.97	1.96	1.87	1.93
$n_{p\sigma}^X$	1.81	1.81	1.65	1.65	1.63	1.64
$n_{p\pi}^X$	3.81	3.84	3.83	3.86	3.87	3.91
$n_{d\sigma}^X$					2.00	2.00
$n_{d\pi}^X$					4.00	4.00
$n_{d\delta}^X$					4.00	4.00
q^{Cu}	0.47	0.64	0.29	0.33	0.27	0.50
n_s^{Cu}	0.48	0.22	0.54	0.31	0.60	0.34
$n_{p\sigma}^{Cu}$	0.10	0.05	0.23	0.12	0.19	0.10
$n_{p\pi}^{Cu}$	0.11	0.11	0.11	0.09	0.11	0.08
$n_{d\sigma}^{Cu}$	1.88	1.93	1.90	1.96	1.93	1.98
$n_{d\pi}^{Cu}$	3.97	4.05	3.94	4.00	3.89	4.00
$n_{d\delta}^{Cu}$	4.00	4.00	4.00	4.00	4.00	4.00
q^C	0.34	0.21	0.37	0.21	0.35	0.21
n_s^C	1.49	1.77	1.45	1.77	1.49	1.77
$n_{p\sigma}^C$	0.95	0.97	0.94	0.97	0.94	0.97
$n_{p\pi}^C$	1.10	0.94	1.11	0.94	1.10	0.94
$n_{d\sigma}^C$	0.03	0.03	0.03	0.03	0.03	0.03
$n_{d\pi}^C$	0.10	0.08	0.09	0.08	0.09	0.08
q^O	−0.20	−0.21	−0.20	−0.21	−0.20	−0.21
n_s^O	1.89	1.82	1.89	1.82	1.90	1.82
$n_{p\sigma}^O$	1.38	1.40	1.38	1.40	1.38	1.40
$n_{p\pi}^O$	2.90	2.96	2.90	2.96	2.90	2.96

Antes et al.[17] predicted the Cl electric field gradients in OCCuCl and CuCl as −1.111 and −1.603 au, respectively. These result in ^{35}Cl coupling constants of −21.2 and −30.5 MHz, respectively, to be compared with the experimental values of −21.5 and −32.1 MHz. The agreement is very reasonable and rather better (especially for the monomer) than that found for the corresponding Au derivatives. (A more recent calculation by Pernpointner et al.[34] gave an EFG of −1.706 au and eQq = −32.5 MHz for the monomer, in much better agreement with experiment.)

Mulliken valence orbital populations were examined in order to gain some insight into the bonding of the molecules. These were provided by Antes et al.[17] for OCCuCl and have been supplemented by analyses for OCCuF and OCCuBr (together with a further analysis of OCCuCl) during this work (Table 9). The calculated trends following the attachment of CO to CuCl are in good agreement with those found by Antes et al. In both studies (and in all molecules), a decrease in electron density in the n_s(C) orbital is the result of complex formation; this is associated with OC→MCl donation. This is accompanied by decreases in the respective populations of the $nd\sigma$ and $nd\pi$ orbitals of the Cu atom and an increase in the $np\pi^*$ population of the carbon atom. The changes in the π-orbital populations are evidence for a degree of ClM→CO back-donation. The most significant decrease in the population of the π-orbitals on the metal atom is seen in the bromide. Antes et al. concluded from their analysis that OC→MCl donation is accompanied by a small degree of ClM→CO back-bonding in OCCuCl. The results of the calculations presented herein on OCCuF and OCCuBr

(34) Pernpointner, M.; Schwerdtfeger, P.; Hess, B. A. *Int. J. Quantum Chem.* **2000**, *76*, 371.

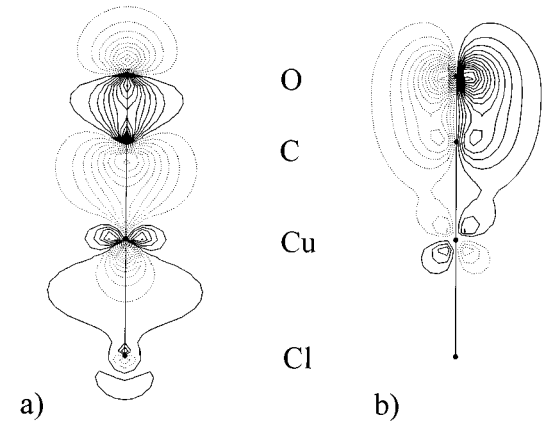

Figure 4. Contour diagrams of the (a) 10σ and (b) 3π molecular orbitals of OCCuCl.

Table 10. ^{63}Cu Nuclear Spin-Rotation Constants and Shielding Parameters

param[a]	$^{16}O^{12}C^{63}CuF$	$^{16}O^{12}C^{63}Cu^{35}Cl$	$^{16}O^{12}C^{63}Cu^{79}Br$
C_I[b]	10.13(16)	6.057(93)	3.57(14)
C_I(nucl)	−0.60	−0.511	−0.52
C_I(elec)	10.73	6.568	4.09
σ_p	−1906(31)	−1732(27)	−1629(63)
σ_d	2511	2540	2613
σ	605	808	984
Ω	2700(43)	2395(36)	2134(81)

[a] Spin-rotation constants are in kHz and shielding parameters in ppm. [b] Measured C_I values from Tables 1−3.

further support this hypothesis. It should be noted, however, that neither of these theoretical studies were based on wave functions that reproduced the experimental geometry to a high degree of precision.

MOLDEN 3.4[35] contour diagrams of two molecular orbitals of OCCuCl are provided in Figure 4. These illustrate the σ- and π-type interactions that are present in the M−C bond and that contribute to the stability of the molecule.

B. ^{63}Cu Nuclear Shielding. The nuclear spin-rotation constants C_I are intimately related to the nuclear shielding constants σ and provide a valuable source of this information when they are unavailable from magnetic resonance experiments (e.g., for quadrupolar nuclei, or for nuclei in unstable molecules). In the present work, the C_I(Cu) values have been used to evaluate the average shieldings σ and the spans of the shieldings Ω for ^{63}Cu in $^{16}O^{12}C^{63}CuF$, $^{16}O^{12}C^{63}Cu^{35}Cl$, and $^{16}O^{12}C^{63}Cu^{79}Br$.

The C_I values were first split into their electronic and nuclear parts using[36]

$$C_I = C_I(\text{elec}) + C_I(\text{nucl}) \tag{9}$$

where C_I(nucl) was calculated from the geometries by

$$C_I(\text{nucl}) = -\left(\frac{2e\mu_N g_I B}{hc}\right)\sum_{i\neq A}\left(\frac{Z_i}{r_{Ai}}\right) \tag{10}$$

where e is the proton charge, μ_N is the nuclear magneton, g_I is the g factor for nucleus A (=^{63}Cu in the present case), B is the rotational constant, and Z_i is the atomic number of nucleus i, located a distance r_{Ai} from nucleus A. The resulting values were subtracted from the experimental C_I values to give C_I(elec) using eq 9; these results are summarized in Table 10.

Similarly, the average shielding σ is the sum of a paramagnetic and diamagnetic part:

$$\sigma = \sigma_p + \sigma_d \tag{11}$$

The paramagnetic part, σ_p, is directly proportional to C_I(elec) according to

$$\sigma_p = -\left(\frac{m_p}{3mg_I B}\right)C_I(\text{elec}) \tag{12}$$

where m_p and m are the masses of the proton and electron, respectively. The σ_p values obtained with the equation are also in Table 10. The diamagnetic part, σ_d, is related to C_I(nucl) by

$$\sigma_d = -\left(\frac{m_p}{3mg_I B}\right)C_I(\text{nucl}) + \sigma_d(\text{atom}) \tag{13}$$

in which σ_d(atom) is the free atom diamagnetic shielding, obtainable from tables,[37] as 2405 ppm for ^{63}Cu. The values of σ_d and resulting values of σ are also in Table 10.

The span Ω is defined by $\Omega = \sigma_{||} - \sigma_{\perp}$, where $\sigma_{||}$ and $\sigma_{\perp}$ are the components of the shielding tensor parallel and perpendicular to the molecular axis, respectively. It can be evaluated directly from the spin-rotation constants C_I using[38]

$$\Omega = \left(\frac{m_p}{2mg_I B}\right)C_I \tag{14}$$

The results for the three molecules are in Table 10.

For the three molecules, both the shieldings and the spans are fairly similar from molecule to molecule, consistent with their similar structures. The spans, which are a measure of the asymmetries of the shieldings, are large, and much bigger than the actual σ values; given that the molecules are linear, this is unsurprising. Although uncertainties, which reflect those of the spin-rotation constants, can be readily assigned to both σ_p and Ω, this cannot be so easily done for σ. The values for σ depend strongly on that of σ_d(atom), which was calculated without considering relativistic effects and should really only be valid for atoms toward the top of the periodic table. Fortunately this is usually found to apply for Cu. Given that good values of σ_d and hence σ have been obtained in other cases,[39] the values obtained should be fairly reliable.

IX. Discussion and Conclusions

Through the assignment of their microwave spectra, it has been shown that OCCuF, OCCuCl, and OCCuBr can be stabilized within a supersonic jet. In each case, the C−O bond

(35) Schaftenaar, G.; MOLDEN 3.4; CAOS/CAMM Center, The Netherlands, 1998.
(36) Flygare, W. H. *J. Chem. Phys.* **1964**, *41*, 793.
(37) Malli, G.; Fraga, S. *Theor. Chim. Acta* **1966**, *5*, 275.
(38) Wasylishen, R. E.; Bryce, D. L.; Evans, C. J.; Gerry, M. C. L. *J. Mol. Spectrosc.* **2000**, *204*, 184.
(39) Müller, H. S. P.; Gerry, M. C. L. *J. Chem. Phys.* **1995**, *103*, 577.
(40) Evans, C. J.; Gerry, M. C. L. *J. Phys. Chem. A*, submitted for publication.
(41) Solupe, M.; Bauschlicher, C. W., Jr.; Lee, T. J. *Chem. Phys. Lett.* **1992**, *189*, 266.
(42) Kasai, Y.; Obi, K.; Ohshima, Y.; Endo, Y.; Kawaguchi, K. *J. Chem. Phys.* **1995**, *103*, 90.
(43) Hedberg, L.; Iijuma, T.; Hedberg, K. *J. Chem. Phys.* **1958**, *70*, 3224.
(44) Beagley, B.; Cruickshank, D. W. J.; Pinder, P. M.; Robiette, A. G.; Sheldrick, G. M. *Acta Crystallogr.* **1969**, *B25*, 737.
(45) Huber, K. P.; Herzberg, G. *Molecular Spectra and Molecular Structure: Constants of Diatomic Molecules*; Van Nostrand: New York, 1979.

Table 11. Bond Lengths of Various Metal Carbonyl Species in Å

	M−C	C−O	comments
OC−CuF	1.765	1.131	$r_{I\epsilon}$ values, this work
OC−CuCl	1.795	1.129	$r_{I\epsilon}$ values, this work
OC−CuBr	1.803	1.128	$r_{I\epsilon}$ values, this work
OC−AuF	1.847	1.134	r_0 values (FTMW, ref 13)
OC−AuCl	1.883	1.132	$r_{I\epsilon}$ values (FTMW, ref 13)
OC−AuBr	1.892	1.132	$r_{I\epsilon}$ values (FTMW, ref 13)
Pt−CO	1.760	1.148	$r_{I\epsilon}$ values, ref 40
Ni−CO	1.687	1.166	CCSD, ref 41
Fe−CO	1.727	1.160	$r_{I\epsilon}$ value, ref 42
Ni−$(CO)_4$	1.838	1.141	electron diffraction, ref 43
Fe−$(CO)_5$	1.833	1.145	electron diffraction, ref 44
CO		1.128	r_e value, ref 45

[a] The $r_{I\epsilon}$ values are given in order to allow comparison with the bond lengths of OC−AuX. The preferred r_m values (Table 5) are up to 0.001 Å shorter.

length is close to that of free CO (1.128 Å). This is in agreement with the trend observed for various OCAuX species.[13] In all cases, the theoretical calculations of Plitt et al.[8] are found to give the best agreement with the experimental geometry. The M−C and C−O bond lengths are compared with those of a range of other metal carbonyls in Table 11. The C−O bond in a given OCCuX species is shorter than that in the analogous OCAuX molecule, by 0.003−0.004 Å. In all the species containing a noble metal atom, this distance is considerably shorter (by at least 0.014 Å) than in PtCO, NiCO, and FeCO. The C−O bond lengths in $Ni(CO)_4$ and $Fe(CO)_5$ are longer than the distances in OCAuX and OCCuX by between 0.01 and 0.016 Å. The M−C bond is shorter in OCCuX than OCAuX by 0.08−0.09 Å yet slightly longer than the distances in PtCO, NiCO, and FeCO. The various OCCuX molecules have M−C bonds that are shorter than those in $Ni(CO)_4$ and $Fe(CO)_5$ by between 0.03 and 0.07 Å.

The vibrational wavenumbers estimated from the measured distortion constants are moderately close to the results of ab initio calculations and especially, for OCCuCl, the CPF calculations performed by Plitt et al.[8] There are significant changes in the nuclear quadrupole coupling constants of Cu, Cl, and Br on the attachment of CO to CuX, suggesting that comparatively strong M−C bonds exist. This conclusion is supported by the Cu−C bond energies of 150 and 143 kJ mol^{-1} calculated earlier for OCCuF[18] and OCCuCl.[16] It is also supported by the results of Mulliken orbital population analyses, which show evidence of π-back-donation from Cu to CO in all the species studied.

Acknowledgment. The research has been supported by the Natural Sciences and Engineering Research Council (NSERC) of Canada and by the Petroleum Research Fund, administered by the American Chemical Society.

Supporting Information Available: Measured rotational transitions of OCCuX (X = F, Cl, Br). This material is available free of charge via the Internet at http://pubs.acs.org.

IC0105967